THE JOURNAL OF BIOLOGICAL CHEMISTRY VOL. 288, NO. 50, pp. 35812–35823, December 13, 2013

25-Hydroxycholesterol Activates the Integrated Stress Response to Reprogram Transcription and Translation in Macrophages*[S]

Received for publication, September 16, 2013, and in revised form, October 28, 2013 Published, JBC Papers in Press, November 4, 2013, DOI 10.1074/jbc.M113.519637

Norihito Shibata,[a,b1] Aaron F. Carlin,[c1] Nathanael J. Spann,[a] Kaoru Saijo,[a] Christopher S. Morello,[a] Jeffrey G. McDonald,[d] Casey E. Romanoski,[a] Mano R. Maurya,[e] Minna U. Kaikkonen,[a] Michael T. Lam,[a] Andrea Crotti,[a] Donna Reichart,[a] Jesse N. Fox,[a] Oswald Quehenberger,[c] Christian R. H. Raetz,[†f] M. Cameron Sullards,[g] Robert C. Murphy,[h] Alfred H. Merrill, Jr.,[g] H. Alex Brown,[i] Edward A. Dennis,[j] Eoin Fahy,[e] Shankar Subramaniam,[a,e,j] Douglas R. Cavener,[k] Deborah H. Spector,[a] David W. Russell,[d] and Christopher K. Glass[a,c2]

From the Departments of [a]Cellular and Molecular Medicine, [e]Bioengineering, [j]Chemistry and Biochemistry, and [c]Medicine, University of California at San Diego, La Jolla, California 92093-0651, the [d]Department of Molecular Genetics, University of Texas Southwestern Medical Center, Dallas, Texas 75390, the [i]Department of Pharmacology, Vanderbilt Institute of Chemical Biology, Vanderbilt University School of Medicine, Nashville, Tennessee 37232-6600, the [f]Department of Biochemistry, Duke University School of Medicine, Duke University Medical Center, Durham, North Carolina 27710, the [h]Department of Pharmacology, University of Colorado at Denver, Aurora, Colorado 80045, the [g]Schools of Biology, Chemistry, and Biochemistry and the Parker H. Petit Institute for Bioengineering and Bioscience, Georgia Institute of Technology, Atlanta, Georgia 30332-0230, the [k]Department of Biology, Penn State University, University Park, Pennsylvania 16802-5301, and the [b]Division of Biochemistry and Molecular Biology, National Institute of Health Sciences, 1-18-1 Kamiyoga, Setagaya-ku, Tokyo 158-8501, Japan

Background: Interferons and viral infections stimulate the production of 25-hydroxycholesterol.
Results: 25-Hydroxycholesterol significantly alters cholesterol ester and sphingolipid levels and activates the integrated stress response.
Conclusion: 25-Hydroxycholesterol activates the GCN2/eIF2α/ATF4 integrated stress response likely by causing cysteine depletion and/or by generating oxidative stress.
Significance: Altering important membrane lipids and activating the integrated stress response may contribute to the antiviral activity of 25-hydroxycholesterol.

25-Hydroxycholesterol (25OHC) is an enzymatically derived oxidation product of cholesterol that modulates lipid metabolism and immunity. 25OHC is synthesized in response to interferons and exerts broad antiviral activity by as yet poorly characterized mechanisms. To gain further insights into the basis for antiviral activity, we evaluated time-dependent responses of the macrophage lipidome and transcriptome to 25OHC treatment. In addition to altering specific aspects of cholesterol and sphingolipid metabolism, we found that 25OHC activates integrated stress response (ISR) genes and reprograms protein translation. Effects of 25OHC on ISR gene expression were independent of liver X receptors and sterol-response element-binding proteins and instead primarily resulted from activation of the GCN2/eIF2α/ATF4 branch of the ISR pathway. These studies reveal that 25OHC activates the integrated stress response, which may contribute to its antiviral activity.

Macrophages and related cell types play key roles in both innate and adaptive immunity. Tissue-resident macrophages function as sentinels that detect invading pathogens through pattern recognition receptors, which activate intrinsic antimicrobial activities and induce the elaboration of cytokines and chemokines that amplify the initial inflammatory response, recruit additional immune cells, and commence acquired immunity (1–3). The interferon (IFN) family of cytokines is a key component of innate immunity and a first line of defense against viral infection. Type I IFNs trigger a signaling cascade resulting in amplification of hundreds of interferon-stimulated genes, many of which have unclear roles in viral immunity (4).

Cholesterol 25-hydroxylase (*Ch25h*) is a recently identified interferon-stimulated gene that encodes an ER[3]-associated glycoprotein that catalyzes the production of 25OHC from cholesterol (5). *Ch25h* is highly induced in macrophages following stimulation with the TLR4 ligand Kdo2 lipid A contemporaneously with secondary response genes that are dependent on type I interferon production (6, 7). 25OHC regulates choles-

* This work was supported, in whole or in part, by National Institutes of Health Grant GM U54 069338 (to the LIPID MAPS Consortium). This work was also supported by the Clayton Foundation for Research (to D. W. R.) and the American Heart Association (to N. S.).
[S] This article contains supplemental Datasets 1–4.
† Deceased.
[1] Both authors contributed equally to this work.
[2] To whom correspondence should be addressed: Depts. of Cellular and Molecular Medicine and Medicine, University of California at San Diego, and Dept. of Cellular and Molecular Medicine, George Palade Labs, Rooms 217 and 219, 9500 Gilman Dr., MC 0651 CMM-W, La Jolla, CA 92093-0651. Tel.: 619-534-6011; Fax: 619-534-8549; E-mail: ckg@ucsd.edu.

[3] The abbreviations used are: ER, endoplasmic reticulum; CE, cholesterol ester; 25OHC, 25-hydroxycholesterol; GO, Gene Ontology; BMDM, bone marrow-derived macrophage; LXR, liver X receptor; SREBP, sterol-response element-binding protein; m.o.i., multiplicity of infection; MCMV, mouse cytomegalovirus; ISR, integrated stress response; EGFP, enhanced GFP; Q-PCR, quantitative PCR; Ab, antibody; 27OHC, 27-hydroxycholesterol; EC, epoxycholesterol; TRAP, translating ribosome affinity purification; 24,25-EC, 24,25-epoxycholesterol.

terol metabolism, acting as a suppressor of cholesterol biosynthesis through inhibition of SREBP proteolytic processing (8), and as a ligand for liver X receptors (LXRs), enabling LXR-mediated induction of genes that encode proteins mediating cholesterol export (9). CH25H and its product 25OHC play roles in regulating both innate and adaptive immunity. Mice lacking *Ch25h* exhibit abnormal immunoglobulin A production by B lymphocytes (6) and dysfunctional B cell migration within follicles (10). Recent studies demonstrated a broad and potent antiviral activity of CH25H and 25OHC (11, 12) and suggested that 25OHC impedes viral infection at multiple stages.

The integrated stress response (ISR) is a shared stress response pathway that can be initiated by the four eIF2α kinases as follows: heme-regulated inhibitor (hRI); protein kinase R (PKR); PKR-like ER kinase (PERK), and general control nonderepressible 2 (GCN2). Each kinase is activated by various sources of cellular stress and phosphorylates eIF2α (13, 14). Phosphorylation of eIF2α rapidly suppresses initiation of protein translation, but paradoxically there is increased production of the transcription factor ATF4 causing induction of certain stress-related genes (15, 16). Together, suppression of protein translation and induction of stress response genes function to either alleviate cellular stress and restore homeostasis or trigger apoptosis if the stress cannot be corrected (17, 18). Additionally, the phosphorylation of eIF2α by PKR and other eIF2α kinases is an important antiviral mechanism that suppresses infection by inhibiting protein translation and stimulating apoptosis (4, 19–21).

To gain further insights into the antiviral activities of 25OHC, we performed lipidomic and transcriptomic analysis of 25OHC-treated bone marrow-derived macrophages (BMDMs). We found that 25OHC treatment significantly altered specific subsets of lipids and activated a robust integrated stress response that reprogrammed macrophage transcription and translation.

EXPERIMENTAL PROCEDURES

Materials—Tissue culture plastic was purchased from Fisher. Tissue culture medium and other tissue culture reagents were obtained from Mediatech Inc. 25OHC and tunicamycin were purchased from Sigma; EC was from Biomol; 27OHC was from Research Plus, Inc., and Kdo2 was from Avanti Polar Lipids. Supplemental amino acids, glutathione, and *N*-acetylcysteine were purchased from Sigma.

Mice and Primary Cells—C57BL/6 thioglycollate-elicited macrophages and bone marrow-derived macrophages were obtained from WT and CH25H KO (6), LXR DKO (22, 23), INSIG2 KO (24), and GCN2 KO (25) mice and cultured as described previously (26). For oxysterol experiments, BMDMs or thioglycollate elicited-macrophages were plated in RPMI 1640 medium supplemented with 10% lipid-reduced FBS (HyClone) for 18 h before treatment. For RNAi experiments in BMDMs, cells were transfected with control or SMARTpool siRNAs (40 nM, Dharmacon) directed against ATF4, HRI, PKR, PERK, GCN2, and Insig-1 by using Lipofectamine 2000 (Invitrogen). Cells were used for experiments after 48 h of incubation, and target gene knockdown was validated by Q-PCR. MCMV infections of primary BMDMs used strain MW97.01 at the indicated multiplicities of infection.

Lipid Measurements—Liquid chromatography/mass spectrometry measurements were performed to measure lipid species following detailed protocols available on line.

Immunoblot Analysis—The BMDMs were lysed in a buffer containing 20 mM HEPES (pH 7.4), 150 mM NaCl, 10% glycerol, 1 mM EDTA, 1% Triton X-100, 100 mM NaF, 100 mM sodium pyrophosphate, 17.5 mM β-glycerophosphate, and 1× complete protease inhibitor mixture (Roche Applied Science), and 1× PhosSTOP phosphatase inhibitor mixture (Roche Applied Science). Each sample (20 μg) was separated by SDS-PAGE and transferred to a polyvinylidene difluoride membrane. The membranes were incubated with anti-eIF2a antibody, anti-phospho-eIF2a antibody, and anti-CHOP antibody (Cell Signaling).

RNA Analysis—Total RNA was purified and analyzed by microarray and quantitative PCR as described previously (27). cDNA was synthesized from 1 μg of total RNA and used for quantitative PCR with gene-specific primers. Mouse *36b4* mRNA was used as an invariant control. PCR primers used were as follows (5′ to 3′): *36b4*, GCT CGA CAT CAC AGA GCA GG and CCG AGG CAA CAG TTG GGT AC; *Ch25h*, CCA TCT TTA CCT TTC ACG TGA TTA AC and CAG CCA AAG GGC ACA AGT CT; *Ddit3*/CHOP, GCA GCG ACA GAG CCA GAA TAA and TGT GGT GGT GTA TGA AGA TGC A; *Chac1*, GGC TTC GTT CGT GGC TAT AGC and CAG CCC TCA CGG TCT TCA AG; *Trib3*, CTT GCG CGA CCT CAA GCT and ATC ACG CAG GCA TCT TCC A; *Atf4*, CTC GGA ATG GCC GGC TAT and GTC CCG GAA AAG GCA TCC T; and *Asns*, GCC ATG ACA GAA GAT GGG TTT C and AAG GGA GTG GTG GAG TGT TTT AAG.

Global Protein Translation—After the indicated cell incubations, the medium was switched to RPMI 1640 without methionine/cysteine. After 60 min, the cells were incubated with EasyTag EXPRESS ^{35}S Protein Labeling Mix (PerkinElmer Life Sciences) at 20 μCi ml^{-1} for 20 min. The cells were then lysed in a buffer containing 50 mM Tris-HCl (pH 7.5), 150 mM NaCl, 1 mM EDTA, 1% Triton X-100, and 1× complete protease inhibitor mixture. Proteins in the lysate were precipitated using trichloroacetic acid, and radioactivity of the precipitated proteins was measured by a scintillation counter.

Translating Ribosome Affinity Purification, Construct Design, and Isolation Protocol—The Csf1r-EGFP-L10a transgenic construct was produced by first subcloning EGFP-L10a fusion protein construct from S296.EGFP-L10a into p3×FLAG-CMV-7.1 (Sigma) at NotI and XbaI sites. The fragment containing 3×FLAG-EGFP-L10a was then subcloned into ApaI and NotI sites of p7.2cfms-egfp thereby replacing the EGFP previously contained in the destination plasmid. The cfms (Csf1r) promoter 3×FLAG-EGFP-L10a transgenic construct was then linearized by digestion with MluI and SalI and utilized for production of transgenic mice in the C57Bl/6 strain. The cell-specific expression of the Csf1r-EGFP-L10a construct was analyzed by flow cytometry. Mouse blood was extracted and anticoagulated with EDTA before blocking with 0.5 μg of anti-CD16/32 Fc Ab (eBioscience) for 30 min at 4 °C. Cells were stained for 30 min on ice in staining buffer containing DPBS + 5% FBS + 5 mM

EDTA using CD115-APC Ab (eBioscience), CD11b-PE (Biolegend) Ab, and Gr1-PECy7 Ab (eBioscience). RBCs were lysed using whole blood lysing reagent kit (Beckman Coulter). Samples were processed and analyzed using an LRSII flow cytometer (BD Biosciences) and FlowJo software. BMDMs (1×10^7) from Csf1r-EGFP-L10a transgenic mice were treated with DMSO, 25OHC, or tunicamycin for the indicated times, and total RNA or translating RNA was isolated by RNeasy (Qiagen) directly or following TRAP, as described previously (28), except that cell scraping in ice-cold lysis buffer containing Nonidet P-40 0.5% was used in lieu of homogenization. Ribosomal RNA was removed from total RNA or TRAP isolated RNA by poly(A) selection as described previously or using Ribo-Zero rRNA removal kit (Epicenter). Ribosome-depleted mRNA was prepared for sequencing as described previously (29). RNA libraries underwent Illumina sequencing at the University of California at San Diego BioGeM Core. Two (tunicamycin) or three (DMSO and 25OHC) independent biological replicates were performed for each treatment.

Gene Ontology and Motif Analysis—Gene Ontology (GO) enrichments for groups of regulated genes were performed using Database for Annotation, Visualization, and Integrated Discovery (DAVID) Version 6.7 (30, 31). *De novo* motif discovery was carried out using Homer software, University of California at San Diego (26). The parameters used were mouse (promoter set), −start −500 −end 100 (promoter region search from −500 bp from transcription start site to +100 bp from transcription start site), −len 8,10,12 (motif length bp). Sequences were searched in both forward and reverse complement orientations.

Virus Experiments—Tissue culture-derived MCMV strain K181 was prepared in BALB/c mouse embryonic cells and titered on NIH 3T3 cells (ATCC CRL 1658) as described previously (32, 33). BMDMs were infected with MCMV at multiplicities of infection ranging from 0.1 to 10 pfu/cell. Virus was adsorbed for 6 h; the inoculum was removed, and the cells were fed with fresh medium. RNA analysis and global protein translation analysis were done as described above. Infectious MCMV was quantified by plaque assay on NIH 3T3 monolayers. Dilutions of the culture medium from the infected BMDMs were adsorbed to the cells in 0.25 ml of DMEM, 5% newborn calf serum (Invitrogen) with occasional agitation. After a 5-h adsorption period, an overlay of 1 ml of DMEM, 5% newborn calf serum and 0.4% agarose was added. Plaques were fixed 5 days later, stained with crystal violet, and counted. Each titer was calculated as the mean titer (pfu/ml) of triplicate infections and a single plaque assay for each infection.

Statistical Analysis—Statistical analyses were performed with two-way analysis of variance test for lipid analysis, with analysis of variance and Bonferroni multiple comparison test for MCMV plaque assay, and with Student's *t* test for other experiments.

RESULTS

25OHC Alters Cholesterol Ester and Sphingolipid Formation—To investigate the effects of 25OHC on macrophages, BMDMs cultured in standard 10% serum-containing media or 10% lipid-deficient serum-containing media plus compactin were treated with 5 μM 25OHC for times ranging from 30 min to 24 h. Lipid and gene expression changes were evaluated by mass spectrometry and microarray analysis, respectively. Culture in lipid-deficient serum (LDS) plus compactin depletes cellular cholesterol, maximally increasing SREBP activity and inhibiting LXR activity as compared with culture under standard conditions. We quantified 569 lipid species in three independent experiments (raw lipid data are available on line at Lipid Maps). Two-way analysis of variance of 25OHC-treated BMDMs identified significant changes in cholesterol ester (CE) and sphingolipids levels (Fig. 1*A*). CE(18:1), CE(16:0), and CE(18:0) were quantitatively the most abundant species to accumulate and exhibited 3–7-fold increases over base-line levels (Fig. 1*B*). Additionally, 25OHC increased ceramide and glucosylceramide levels while decreasing sphingomyelins, primarily at late time points of 12 and 24 h (Fig. 1*A*). The majority of 25OHC-dependent changes in CE and sphingolipid levels occurred in BMDMs cultured in both standard 10% serum-containing media and 10% LDS-containing media (Fig. 1*A*).

25OHC Suppresses SREBPs, Activates LXRs, and Induces Stress Response Genes—Parallel analysis of the macrophage transcriptome demonstrated the expected changes in SREBP and LXR target genes in response to both alterations in media lipid content and treatment with 25OHC (Fig. 1*C* and supplemental Dataset S1). Culture in LDS caused induction of *Hmgcr* mRNA levels (Fig. 1*D*), although 25OHC suppressed *Hmgcr* mRNA levels and induced *Abca1* (Fig. 1, *C* and *D*). Larger magnitude differences in SREBP and LXR (*Hmgcr* and *Abca1*)-regulated genes were notable in BMDMs grown in LDS + compactin, as these conditions maximally activate SREBPs and repress LXRs prior to treatment with 25OHC (Fig. 1*C*). In light of the robust effects of 25OHC on SREBP and LXR target genes, the effects of 25OHC on the lipidome are more selective than would be expected, suggesting roles of post-transcriptional mechanisms in the maintenance of lipid homeostasis.

LXRs are the only known targets of 25OHC that directly induce gene expression; however, the majority of 25OHC-stimulated genes identified in the transcriptional analysis are not established LXR targets. In fact, the up-regulated set of genes was most significantly enriched for functional annotations related to ER to Golgi transport and response to ER stress (Fig. 2*A*). *Atf4*, *Chop/Ddit3*, *Chac1*, *Trib3*, and asparagine synthetase (*Asns*) are up-regulated during cellular responses to stress and were among the most highly induced genes by 25OHC (Fig. 1*C* and supplemental Dataset S1) (13, 34). Q-PCR assays in BMDMs confirmed that stress response genes were induced by 25OHC in a concentration- and time-dependent manner (Fig. 2, *B* and *C*).

MCMV Infection Stimulates 25OHC Production and Induces Stress Response Gene Transcription—*Ch25h* is an interferon-stimulated gene, and two recent independent publications demonstrated that CH25H and its product 25OHC have broad antiviral activity (11, 12). To determine whether the concentrations of 25OHC produced during viral infections were capable of inducing ISR genes, we infected BMDMs with MCMV. Consistent with previous findings, we independently found that 25OHC suppressed MCMV infection of BMDMs at various m.o.i. (Fig. 2*D*). Infection with MCMV strongly activated

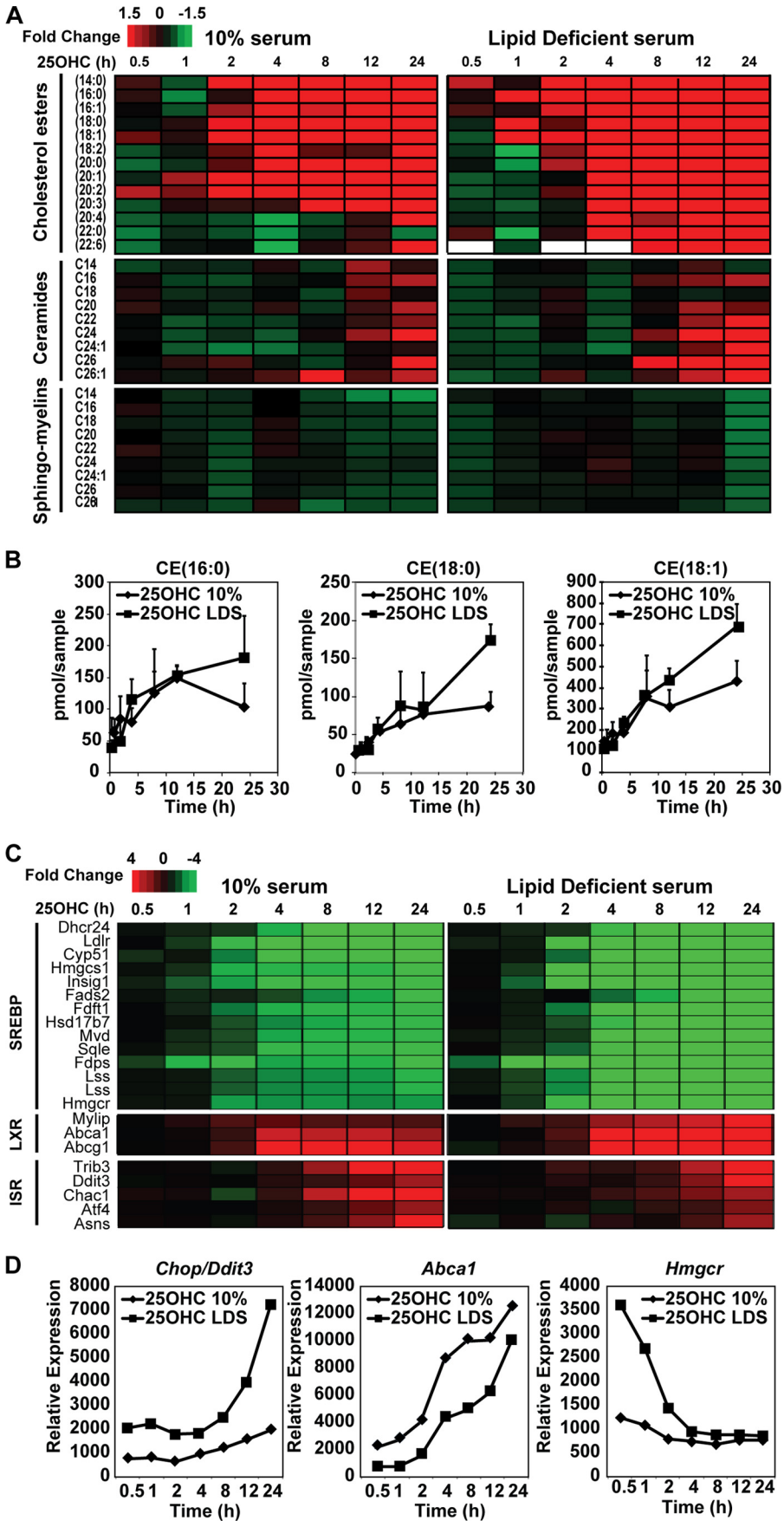
A
Fold Change
1.5 0 -1.5
10% serum
Lipid Deficient serum
25OHC (h)
0.5 1 2 4 8 12 24
Cholesterol esters
(14:0)
(16:0)
(16:1)
(18:0)
(18:1)
(18:2)
(20:0)
(20:1)
(20:2)
(20:3)
(20:4)
(22:0)
(22:6)
Ceramides
Sphingo-myelins
C14
C16
C18
C20
C22
C24
C24:1
C26
C26:1
B
CE(16:0)
CE(18:0)
CE(18:1)
25OHC 10%
25OHC LDS
pmol/sample
Time (h)
C
Fold Change
4 0 -4
10% serum
Lipid Deficient serum
25OHC (h)
SREBP
Dhcr24
Ldlr
Cyp51
Hmgcs1
Insig1
Fads2
Fdft1
Hsd17b7
Mvd
Sqle
Fdps
Lss
Lss
Hmgcr
LXR
Mylip
Abca1
Abcg1
ISR
Trib3
Ddit3
Chac1
Atf4
Asns
D
Chop/Ddit3
Abca1
Hmgcr
25OHC 10%
25OHC LDS
Relative Expression
Time (h)

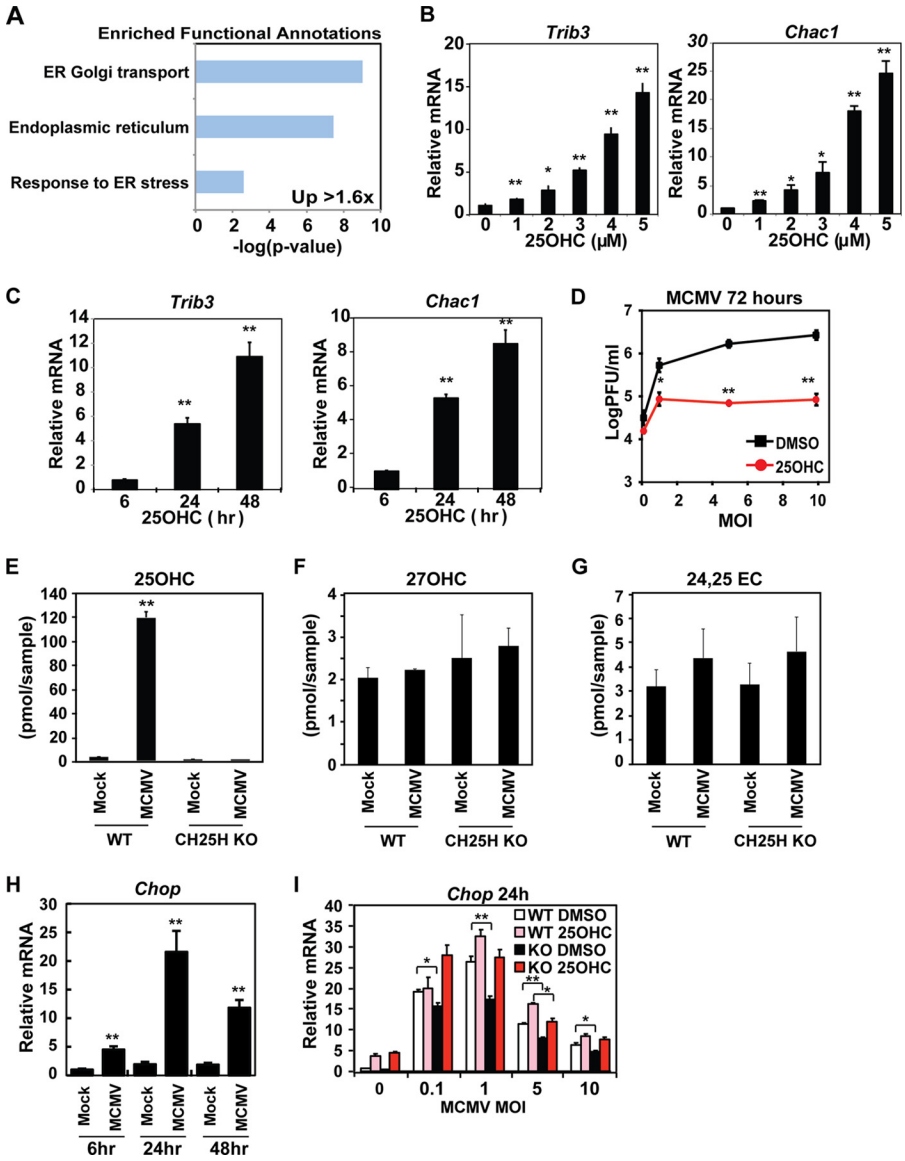

FIGURE 2. **25OHC induces stress related genes.** *A,* GO terms significantly enriched in up-regulated genes in BMDMs treated with 25OHC (*versus* DMSO solvent) for 24 h. Benjamini-corrected −log *p* values are shown. Expression of *Trib3* and *Chac1* mRNAs in BMDMs were treated with 25OHC at increasing doses for 24 h (*B*) or were treated with fixed 25OHC concentration (5 μM) measured over increasing times (*C*). *D,* BMDMs were infected with MCMV (m.o.i. = 0.1, 1, 5, 10) ± 25OHC (5 μM) for 72 h, and the yield of cell-free virus was determined by plaque assay. Data are plotted as mean values ± S.D. For each group, $n = 3$. *, $p < 0.05$, or **, $p < 0.01$ compared with control. Cellular content of 25OHC (*E*), 27OHC (*F*), or 24,25-EC in WT or CH25H KO BMDMs infected with MCMV (m.o.i. = 3) (*G*) for 24 h. *H,* expression of *Chop* mRNA in BMDMs infected with MCMV (m.o.i. = 3) for the indicated time. *I,* expression of *Chop* mRNA in WT or CH25H KO BMDMs infected with MCMV in the presence or absence of 25OHC for 24 h at the indicated m.o.i.. Unless otherwise indicated, data are plotted as mean values ± S.E. For each group, $n = 3$. *, $p < 0.05$, or **, $p < 0.01$.

Ch25h-dependent 25OHC production (Fig. 2*E*). There were no increases in the production of other measurable oxysterols, exemplified by 27OHC and 24,25-epoxycholesterol (24,25-EC) (Fig. 2, *F* and *G*). MCMV infection had no significant effect on total cholesterol (free + esterified) but had divergent effects on desmosterol and 7-dehydrocholesterol in both WT and CH25H KO BMDMs (data not shown). As desmosterol and 7-dehydrocholesterol are the last intermediates of the Bloch and Kandutsh-Russel pathways of cholesterol biosynthesis, respectively, these results suggest complex effects of MCMV infection on late stages of cholesterol biosynthesis.

BMDMs infected with MCMV showed significant induction of *Chop* at 6, 24, and 48 h (Fig. 2*H*). Increases in *Chop* mRNA were partially dependent on endogenous synthesis of 25OHC as WT BMDMs had significantly more *Chop* mRNA when compared with CH25H KO BMDMs (Fig. 2*I*). The decrease in *Chop* induction in CH25H KO macrophages was rescued by exogenous treatment with 25OHC (Fig. 2*I*). MCMV, like

FIGURE 1. **Lipidome and transcriptome analysis in 25OHC-treated BMDMs.** *A,* heat map of CE and sphingolipid changes. *B,* cellular content of the indicated CE in *A*. *C,* transcriptional profiling in BMDMs treated with 5 μM 25OHC for 0.5, 1, 2, 4, 8, 12, and 24 h. *D,* indicated gene expression changes from transcriptomic analysis in *C*. *A* and *C,* log2-based transformation on ratio fold change values are used, where *red shading* indicates up-regulation and *green* indicates down-regulation. *B* and *D,* data are plotted as mean values ± S.E. For each group, $n = 3$.

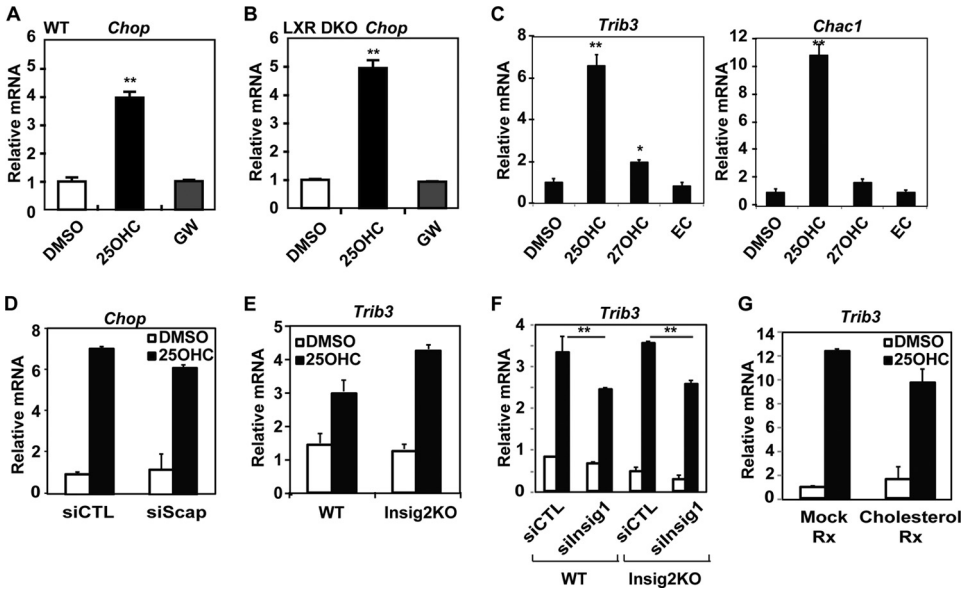

FIGURE 3. **25OHC induces stress-related genes independently of LXRs and SREBPs.** *A,* expression of *Chop* mRNA in WT, or *B,* LXR-deficient BMDMs treated with 25OHC (5 μM) or the LXR-specific agonist GW3965 (1 μM) for 24 h. *C,* expression of *Trib3* and *Chac1* mRNA in BMDMs treated with (5 μM) of the indicated oxysterols for 24 h. *D,* expression of *Chop* mRNA in BMDMs ± *Scap* knockdown treated with 25OHC (5 μM) for 24 h. Expression of *Trib3* mRNA in WT and Insig2 KO BMDMs treated with 25OHC (5 μM) for 24 h without (*E*) or with (*F*) concurrent knockdown of Insig1. *G,* expression of *Trib3* mRNA in BMDMs treated with 5 μM of 25OHC ± 10 μg/ml of cholesterol for 24 h. For experiments in *E* and *F*, each group represents samples from two separate experiment, $n = 6$. *, $p < 0.01$ siCTL compared with si*Insig1* treatment. For all other experiments, data are plotted as mean values ± S.E. For each group, $n = 3$, and *, $p < 0.05$, and **, $p < 0.01$ compared with control.

human cytomegalovirus, stimulates multiple stress response pathways during infection that likely account for the 25OHC-independent elevations in Chop mRNA (35, 36). Thus, macrophage production of 25OHC during MCMV infection contributes to, but is not solely responsible for, stress gene activation during MCMV infection of macrophages.

25OHC Induction of Stress Response Genes Is Independent of LXRs and SREBPs—We next investigated potential roles of LXRs in mediating induction of stress response genes by 25OHC. Treatment of macrophages with the synthetic LXR agonist GW3965 did not stimulate stress response gene expression (Fig. 3*A*). Additionally, 25OHC induced stress response genes in LXR DKO macrophages (Fig. 3*B*). Furthermore, increases in stress gene transcription were significantly greater in response to 25OHC than 27OHC or 24,25-epoxycholesterol (EC), which are also LXR agonists (Fig. 3*C*). These results indicate that 25OHC activates stress response genes independently of LXRs.

SREBP processing and the resulting transcriptional activity are regulated by the INSIGs and SCAP proteins (37). SCAP is required for transport of SREBPs from the ER to Golgi for proteolytic processing. INSIGs are directly bound by oxysterols, causing them to interact with SCAP and sequester SREBPs in the ER (8). Knockdown of Scap using siRNAs did not alter 25OHC induction of stress response genes (Figs. 3*D* and 7*A*), indicating that this effect is independent of SREBP processing. We next investigated possible SREBP-independent roles of Insigs by performing loss of function experiments. BMDMs from INSIG2 KO mice showed similar stress response gene induction by 25OHC compared with WT BMDMs (Figs. 3*E* and 7*B*). We detected a small but significant reduction of 25OHC-dependent stress response gene induction in both WT and INSIG2 KO BMDMs in which *Insig1* was knocked down (Figs. 3*F* and 7*B*). The effect of knocking down INSIG1 is similar irrespective of the presence of INSIG2 even though binding of 25OHC to INSIG2 is sufficient to block SREBP processing. This suggests that INSIG1 partially contributes to 25OHC-dependent stress response gene induction independent of its effects on SREBP processing.

Combined actions of 25OHC on LXR and SREBP can reduce cellular cholesterol levels by simultaneously suppressing cholesterol synthesis and promoting cholesterol efflux. To determine whether cholesterol depletion was responsible for induction of stress response genes, we treated macrophages with 25OHC in the presence and absence of exogenous supplementary cholesterol. The addition of exogenous cholesterol did not significantly inhibit the induction of stress response genes in 25OHC-treated macrophages (Fig. 3*G*).

25OHC Activates the GCN2/eIF2α/ATF4 Branch of the Integrated Stress Response—ATF4 and eIF2α integrate signals from four eIF2α kinases (HRI, PKR, PERK, and GCN2), each of which responds to diverse stress signals, to activate a shared stress response pathway called the ISR. During the ISR, eIF2α is phosphorylated on serine 51 resulting in suppression of *de novo* protein synthesis and induction of ATF4-dependent stress response genes that together function to alleviate cell stress (13).

BMDMs treated with 25OHC significantly increased levels of eIF2α phosphorylation and CHOP protein levels (Fig. 4*A*). Elevations in phosphorylated eIF2α occur in a time-dependent manner with small increases in phosphorylation as early as 8 h and maximal phosphorylation occurring after 16–24 h (Fig. 4*B*). Additionally, 25OHC was the only oxysterol that consistently increased eIF2α phosphorylation (Fig. 4*C*). Phosphorylation of eIF2α inhibits GTP recycling in the ternary complex, eIF2-GTP-tRNA^{Met}, thereby suppressing initiation of protein

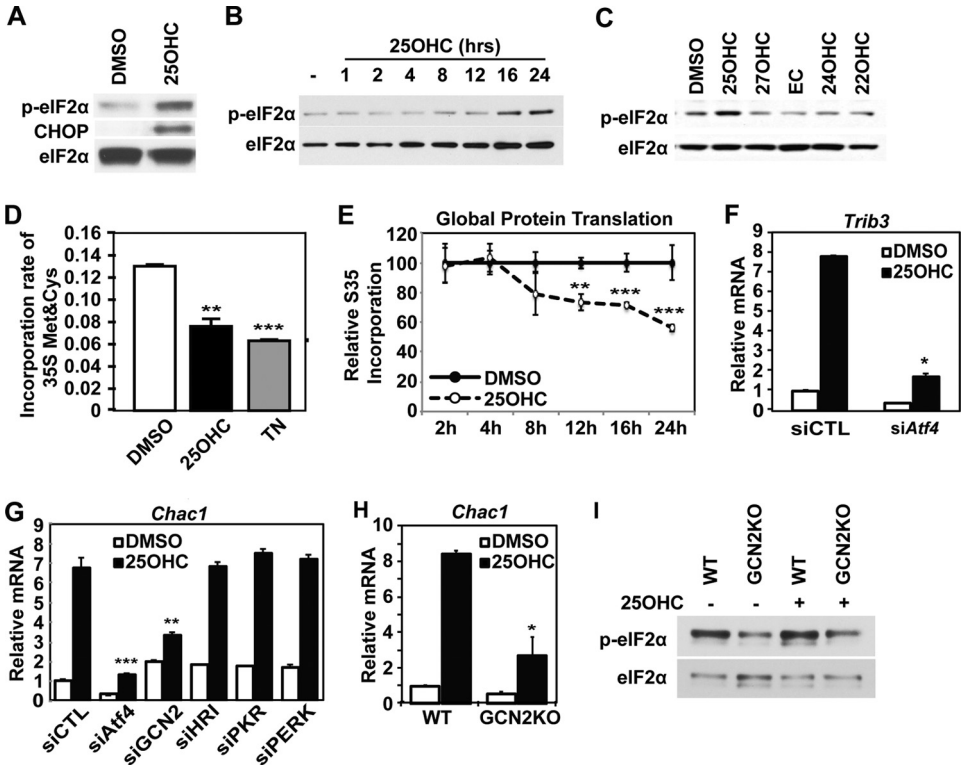

FIGURE 4. **25OHC activates the GCN2/eIF2α/ATF4 branch of the integrated stress response.** *A–C,* protein levels of eIF2α, phosphorylated eIF2α (*p-eIF2α*), and CHOP in BMDMs treated with 25OHC (5 μM), DMSO, or indicated oxysterols (5 μM) for 24 h, or for the indicated times. *D* and *E,* incorporation of pulse-labeled [^{35}S]methionine-cysteine into newly translated proteins in BMDMs treated with tunicamycin (*TN*) (2.5 μg/ml) for 6 h or 25OHC (5 μM) and DMSO for 24 h, or for indicated times. *F,* expression of *Trib3* in BMDMs with knockdown of *Atf4* treated with 25OHC (5 μM) or DMSO for 24 h. *G,* expression of *Chac1* mRNA in BMDMs with knockdown of eIF2α kinases *Eif2ak4*/GCN2, *Eif2ak1*/HRI, *Eif2ak2*/PKR, and *Eif2ak3*/PERK treated with 25OHC (5 μM) or DMSO for 24 h. *H,* expression of *Chac1* mRNA in WT or GCN2 KO BMDMs treated with 25OHC (5 μM) or DMSO for 24 h. *I,* protein levels of eIF2α and phosphorylated eIF2α (*p-eIF2α*) in WT and GCN2 KO BMDMs treated with 25OHC (5 μM) or DMSO for 24 h. Data are plotted as mean values ± S.E. For each group, $n = 3$. *, $p < 0.05$; **, $p < 0.01$; ***, $p < 0.001$ compared with control.

translation. Relatively small increases in eIF2α phosphorylation can significantly inhibit protein translation as its target eIF2β is present in cells at relatively low concentrations (38). BMDMs treated with 25OHC showed depressed levels of active protein translation comparable with the well known ER stress inducer, tunicamycin (Fig. 4*D*). The kinetics of *de novo* protein synthesis inhibition in response to 25OHC occurred maximally at later time points consistent with the time-dependent phosphorylation of eIF2α (Fig. 4*E*).

Phosphorylation of eIF2α during the ISR paradoxically increases ATF4 protein levels due to preferential ATF4 translation with or without increases in *Atf4* transcription leading to increased transcriptional activity at ATF4 target genes (16, 39). Targeted knockdown of *Atf4* significantly reduced induction of stress response genes by 25OHC demonstrating that full transcriptional activation of these genes by 25OHC is ATF4-dependent (Figs. 4*F* and 7*C*).

Four eIF2α kinases (HRI, PKR, PERK, and GCN2) recognize diverse forms of cell stress and trigger the ISR by phosphorylating eIF2α and activating ATF4 signaling (13). Knockdown of the eIF2α kinases in BMDMs suggested that GCN2 was primarily responsible for 25OHC-dependent activation of stress-related genes (Figs. 4*G* and 7*D*). Consistently, BMDMs from GCN2KO mice showed significantly decreased transcription of stress-related genes and eIF2α phosphorylation following 25OHC treatment (Fig. 4, *H* and *I*). The response to 25OHC in GCN2KO macrophages was not abolished, however, suggesting redundancy in ISR activation pathways that can be seen with overlapping stress stimuli (14).

25OHC Reprograms Transcription and Translation—To further investigate effects of 25OHC on translation, we generated transgenic mice expressing EGFP-ribosomal protein L10a under the transcriptional control of Csf1r regulatory elements (Fig. 5*A*). As described previously for the Csf1r-EGFP mouse (40), the expression pattern of the EGFP-L10a fusion protein in the Csf1r-EGFP-L10a mouse is restricted to the myeloid lineage as demonstrated by detection of GFP only in CD11b$^+$ and CD115$^+$ cells (Fig. 5, *B* and *C*). We detected GFP expression in both mononuclear cells (CD115$^+$) and granulocytes (CD115^{low} Gr1$^+$) (Fig. 5, *D* and *E*). The EGFP-L10a system allows efficient isolation of polysomes containing mRNA undergoing active translation using a method termed TRAP (28). By using TRAP, we isolated sufficient quantities of mRNA undergoing active translation from BMDMs to perform RNA-Seq analysis. In parallel, RNA-Seq analysis was performed on total RNA. Relative changes in normalized tag counts for each RefSeq transcript identified by both TRAP and total RNA-Seq are shown in Fig. 6*A*, plotted without (*left scale bar*) or with (*right scale bar*) an estimated correction (40%) for the global effect of 25OHC on translation. Genes shown to be induced by ATF4 and CHOP during the ER stress response demonstrated significantly increased transcription and translation in response to 25OHC

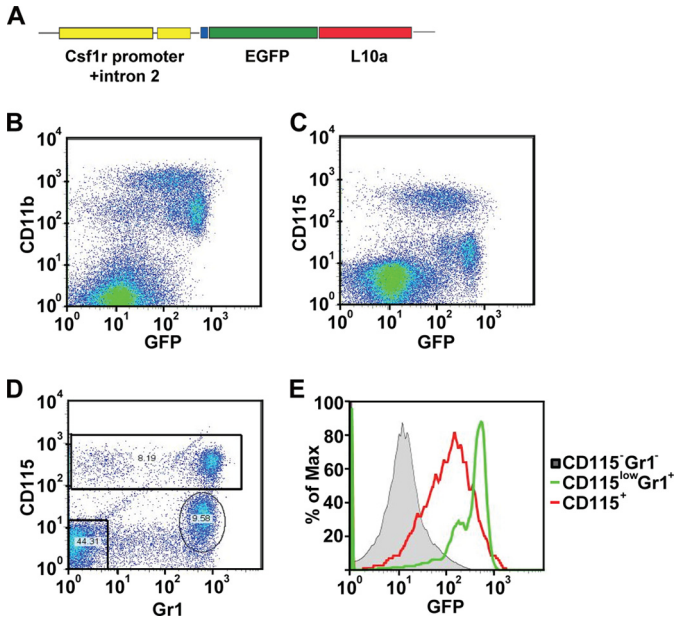

FIGURE 5. **Csf1r-EGFP-L10a mice express the fusion protein in monocytes and granulocytes.** *A,* schematic depiction of Csf1r-EGFP-L10a transgenic construct containing the Csf1r promoter, including intron, three FLAG repeats, and EGFP-L10a fusion protein. Mouse blood was analyzed for the coexpression of GFP with CD11b (*B*) or CD115 (*C*). Coexpression of Gr1 and CD115 (*D*) with subpopulation analysis of GFP expression in $CD115^{+}$ monocytes or $CD115^{low}$ $Gr1^{+}$ granulocytes or $CD115^{-}Gr1^{-}$ cells (*E*).

treatment (Fig. 6*B*) (41). The transcriptional and translational effects of 25OHC on ATF4 and CHOP targets were similar but less robust than effects seen following treatment with tunicamycin, which is known as a potent inducer of ER stress (Fig. 6*B*). 25OHC significantly increased the total mRNA of 455 genes and translating mRNA of 66 genes, with 46 genes significantly up-regulated both transcriptionally and translationally (Fig. 6*C*). As this analysis does not correct for global effects on translation, transcripts undergoing decreased translation are underrepresented, and those undergoing increased translation are over-represented. GO analysis of genes translationally up-regulated >1.5-fold were enriched for functional annotations related to response to ER stress, amino acid activation, and protein transport (Fig. 6*E*). Multiple ISR genes, including *Trib3*, *Ddit3*/*Chop*, *Asns*, *Atf4,* and *Ppp1r15a/Gadd34,* were among the top 100 transcriptionally and top 66 translationally up-regulated genes (supplemental Dataset S2 and S3). Analysis of total and TRAP-isolated mRNA revealed transcriptional suppression of 670 genes and decreased translation of 205 genes in 25OHC-treated BMDMs, with 109 genes down-regulated both transcriptionally and translationally (Fig. 6*D*). Thus, even without correction for global translation, 25OHC down-regulates 205 genes compared with up-regulation of only 66 genes at the translational level, which is consistent with a predominantly suppressive effect on protein translation. GO analysis of translationally suppressed genes >1.5-fold showed enrichment for functional annotations related to the immune and inflammatory responses (Fig. 6*E*). *Ldlr* and *Dhcr24* genes were among the top 10 transcriptionally down-regulated genes consistent with the known suppression of SREBP processing by 25OHC (supplemental Dataset S4) (42).

Based on our experiments, GCN2 is the primary stress response kinase responsible for activating the ISR in macrophages following 25OHC treatment. GCN2 primarily recognizes the stress of amino acid limitation but can be activated by UV irradiation, proteasome inhibition, and some viral infections, although the mechanism by which these stimuli activate GCN2 are less clear (43–45). GO analysis of 25OHC-induced genes identified enrichments in tRNA aminoacylation/amino acid activation. Additionally, we found significant induction of *Atf4*, *Asns*, *Cebpb*, *Ddit3*, *Slc38a2*, *Slc7a1*, and *Trib3*, which are all genes known to be up-regulated in response to amino acid deprivation that carry an amino acid response element bound by ATF4 (46). These findings are consistent with the idea that 25OHC activates the amino acid deprivation stress response via activation of GCN2. To test if amino acid limitation was responsible for 25OHC-dependent GCN2 activation, we supplemented BMDMs with amino acids, including cysteine whose insufficiency has previously been shown to trigger GCN2 to activate the ISR (47). BMDMs supplemented with L-cysteine during treatment with 25OHC showed a significant decrease in transcription of stress-related genes, whereas supplementation with L-asparagine or L-alanine had no effect (Fig. 6*F*). Our transcriptional analysis of 25OHC-treated macrophages showed significant up-regulation of *Asns*, *Cars*, *Cebpb*, *Cebpg*, *Gadd45a*, and *Trib3,* all of which were previously shown to be induced genes in response to cysteine deprivation in HepG2/C3a cells (46).

ATF4 induces genes important for amino acid import, glutathione biosynthesis, and resistance to oxidative stress. We performed *de novo* motif analysis of promoters of genes significantly induced by 25OHC and identified the Nrf2 (*NFE2L2*) motif as the most highly enriched motif (Fig. 6*G*). Nrf2 is a major regulator of the antioxidant response that is activated under conditions of oxidative stress, dimerizes with ATF4 and other bZIP transcription factors, and binds to antioxidant-responsive element sites in the promoters of target genes (48, 49).

In addition to serving as an essential sulfur-containing amino acid, cysteine is also a precursor for the biosynthesis of glutathione (44). The capacity of cysteine to act as a precursor for glutathione, the importance of the ISR in alleviating oxidative stress, and our motif analysis identifying Nrf2, a master regulator activated by oxidative stress, together led us to test whether treatment with anti-oxidants could reduce ISR gene transcription. BMDMs treated with either glutathione or *N*-acetylcysteine showed an almost complete loss of ISR gene induction in response to 25OHC (Fig. 6*H*). Knockdown efficiencies for each siRNA experiment are included as Fig. 7, *A–D*.

DISCUSSION

The lipidomic and transcriptomic analysis of 25OHC-treated macrophages identified significant alterations in select subsets of lipid species, including cholesterol esters and sphingolipids and the unexpected activation of the integrated stress response pathway. Activation of the ISR was specific to 25OHC, compared with other oxysterols, and this effect was independent of the known effects of 25OHC on SREBP processing and LXR activation. We independently corroborated recent publications demonstrating the antiviral activity of 25OHC and

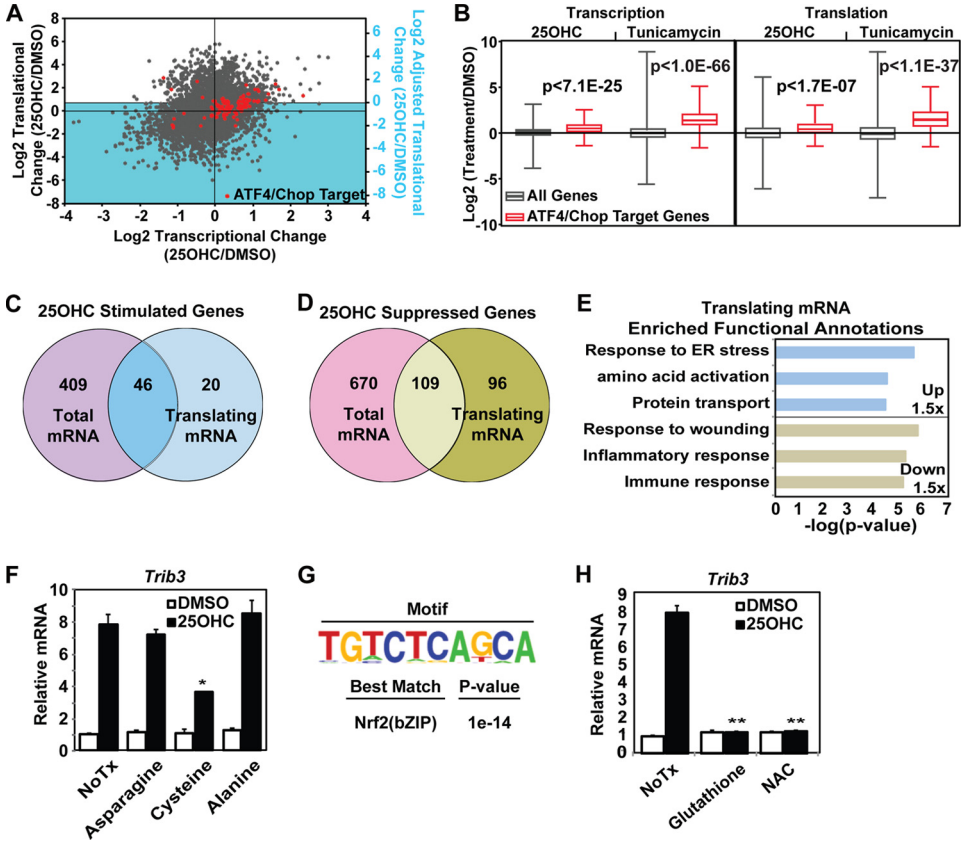

FIGURE 6. **25OHC reprograms macrophage transcription and translation.** *A,* ratio of transcriptional (total mRNA) and translational (TRAP mRNA) change in BMDMs treated with or without 25OHC (5 μM) for 24 h. *Black* and *red dots* correspond to Refseq ATF4 and CHOP target transcripts (41), respectively. Data were plotted without (*left scale bar*) or with (*right scale bar, blue shading*) an estimated correction (40%) for the global suppressive effect of 25OHC on translation. *B,* RNA-Seq-determined transcriptional and translational expression levels comparing all genes (*gray*) with AT4 and CHOP target genes (*red*) in BMDMs treated with 25OHC or tunicamycin. *p* values are from one-tailed *t* tests comparing all genes with ATF4 and Chop target genes. *Venn diagram* of transcriptionally and translationally up-regulated (*C*) and down-regulated (*D*) genes (>1.5×) and their overlap following 25OHC treatment of BMDMs. *E,* GO terms associated with genes up-regulated or down-regulated (>1.5×) at the translational level. *F,* expression of *Trib3* mRNA in WT BMDMs treated with 25OHC (5 μM) or DMSO ± (1 mM) L-cysteine, L-asparagine, or L-alanine for 24 h. *G,* promoter motifs identified by *de novo* motif analysis of the promoters (interval from −500 to +100 bp from the TSS) of genes transcriptionally up-regulated >1.5× by 25OHC. *H,* expression of *Trib3* mRNA in WT BMDMs treated with 25OHC (5 μM) or DMSO ± glutathione (15 mM) or *N*-acetylcysteine (15 mM) for 24 h. Unless otherwise indicated, data are plotted as mean values ± S.E. For each group, $n = 3$. *, $p < 0.05$; **, $p < 0.01$ compared with control.

showed that endogenously produced 25OHC contributes to activation of ISR genes during MCMV infection. Furthermore, 25OHC activates the ISR primarily by triggering the eIF2α kinase GCN2. This activation can be suppressed by cysteine supplementation and addition of antioxidants suggesting that 25OHC stimulates the ISR by altering amino acid metabolism and/or increasing oxidative stress in macrophages.

The observation of dramatic increases in cholesterol ester formation is consistent with previous studies indicating that 25OHC causes recycling of membrane cholesterol to the ER (50, 51). The basis for the increase in ceramides and decrease in sphingomyelins is not yet clear. Sphingomyelin biosynthesis involves CERT-dependent transport of ceramide from the ER to Golgi, which might be disrupted by the ISR or perhaps by 25OHC itself because the transport protein has been shown to be inhibited by isoprenoids (liminoids) (52). In addition, under some conditions, cholesterol depletion can suppress *de novo* sphingomyelin production (53). Sphingomyelin might also decrease due to turnover in ceramide, which is elevated by reactive oxygen species (54). This effect apparently depends on the cell type because an opposite effect (decreased ceramides and increased sphingomyelins) has been reported for CHO cells (55). Further studies will be required to determine the mechanism for these changes.

In addition to its classical functions of suppressing SREBP processing and activating LXRs, 25OHC activated the GCN2/eIF2α/ATF4 branch of the ISR causing global transcriptional and translational reprogramming in the macrophage. The precise trigger by which 25OHC activates GCN2 remains to be established, but it appears to involve increases in oxidative stress and/or depletion of specific amino acids, including cysteine. Activation of the ISR by GCN2 is an important protective mechanism against both oxidative stress and amino acid limitation (44). The amino acid cysteine occupies an interesting position at the interface of amino acid metabolism and oxidative stress as it serves as both an amino acid required for efficient protein synthesis and as a precursor for thiol-containing peptides and proteins, like glutathione, involved in redox reactions. GCN2 is activated by uncharged tRNAs present during amino acid deficiency; however, the mechanism by which GCN2 is activated by other stimuli such as UV radiation or oxidative stress is unclear (25, 56). Cysteine is extremely unstable, and the majority of intracellular cysteine is incorporated into glutathione, which serves as the major storage site of intra-

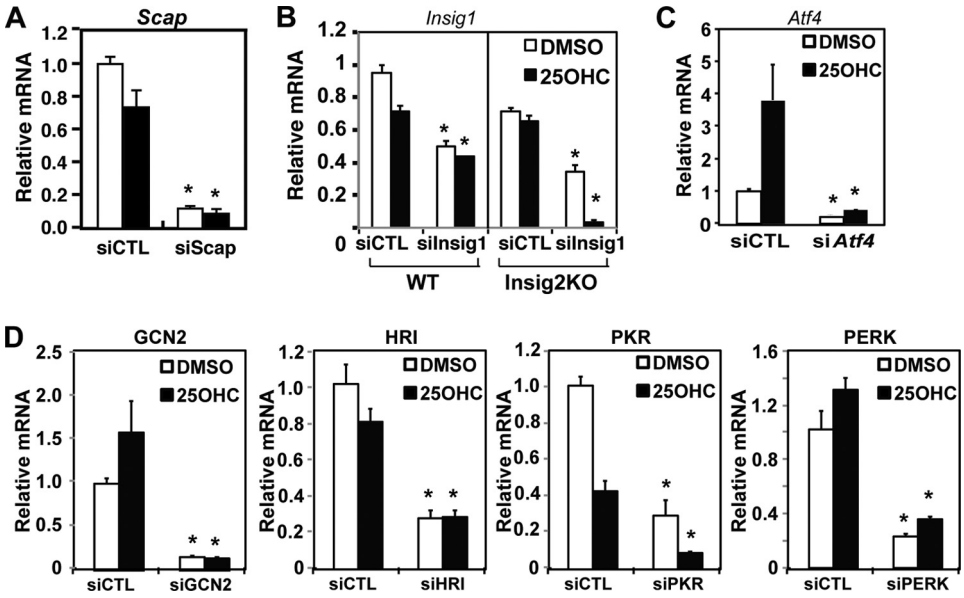

FIGURE 7. **Knockdown efficiency of siRNA experiments.** *A,* expression of *Scap* mRNA in BMDMs in which *Scap* has been knocked down using *Scap*-specific siRNAs treated with 5 μM of 25OHC or DMSO for 24 h. *B,* expression of *Insig1* mRNA in WT and Insig2 KO BMDMs in which *Insig1* has been knocked down using *Insig1*-specific siRNAs treated with 5 μM 25OHC or DMSO for 24 h. *C,* expression of *Atf4* mRNA in BMDMs in which *Atf4* has been knocked down using *Atf4*-specific siRNAs treated with 5 μM 25OHC or DMSO for 24 h. *D,* expression of eIF2α kinase mRNA in BMDMs in which eIF2α kinases have been individually knocked down with specific siRNA to *Eif2ak4*/GCN2, *Eif2ak1*/HRI, *Eif2ak2*/PKR, and *Eif2ak3*/PERK and treated with 5 μM 25OHC or DMSO for 24 h as determined by Q-PCR and normalized to *36B4* expression. For experiments in *B,* each group represents samples from two separate experiment, $n = 6$. *, $p < 0.01$ siCTL compared with si*Insig1* treatment. Data are plotted as mean values ± S.E. For all other experiments, data are plotted as mean values ± S.E. For each group, $n = 3$. *, $p < 0.01$ compared with siCTL treatment.

cellular cysteine (57, 58). One potential mechanism by which GCN2 could recognize increasing oxidative stress would be to recognize a deficiency in intracellular cysteine that develops as levels of glutathione are depleted. Our analysis provides initial evidence suggesting that oxidative stress and/or cysteine limitation is important for 25OHC-mediated activation of GCN2. However, additional studies will be needed to determine the exact stress signal to which GCN2 is responding.

Although two recent independent studies demonstrated the broad antiviral activity of 25OHC, the mechanism by which 25OHC suppresses viral infection is still unclear (11, 12, 59). We demonstrate that 25OHC significantly alters important plasma membrane lipid species and activates the ISR, both of which may contribute to the antiviral activity of 25OHC.

Experiments described by Liu *et al.* (12) suggest that inhibition of viral entry is a major mechanism by which 25OHC suppresses viral infection. Our lipidomic analysis demonstrated large increases in cholesterol esters consistent with significant recycling of membrane cholesterol to the ER and decreases in sphingomyelin. Cholesterol and sphingomyelin are the major components of plasma membrane microdomains, also referred to as "lipid rafts." As many viruses rely on membrane microdomains for entry, alterations in plasma membrane cholesterol or sphingomyelins disrupt membrane microdomains and interfere with viral infectivity (60–62). As 25OHC significantly modifies both plasma membrane cholesterol and sphingomyelin, it likely modifies membrane microdomains, and this may account for the 25OHC-dependent inhibition of viral entry previously described.

Increasing evidence suggests that substantial cross-talk exists between innate immune signaling and the stress response pathways (63). Viruses rely on host metabolic functions, including protein synthesis for survival and propagation (64). Activation of the ISR during viral infection is an important innate immune mechanism that can inhibit some but not all viral infections by suppressing protein translation (4, 64). Consistent with this idea, activation of GCN2 is an important protective immune response to both intracellular bacterial and viral infections (43, 65–67). Our studies demonstrate that 25OHC treatment of macrophages activates GCN2 causing suppression of protein synthesis and that endogenous production of 25OHC by *CH25H* during MCMV infection contributes to ISR gene induction in macrophages. Activation of GCN2 by 25OHC may contribute to its antiviral properties against certain viruses.

Acknowledgments—We thank Dr. Joseph Goldstein (University of Texas Southwestern Medical Center) for critical comments regarding 25OHC, Dr. David Hume (Roslin Institute) for providing the p7.2cfms-egfp plasmid, and Nathaniel Heintz (The Rockefeller University) for the S296.EGFP-L10A plasmid. Microarray analysis, RNA-Seq, and ribosome-protected RNA sequencing were carried out by BioGem at the University of California, San Diego. Transgenic mouse generation was performed at the Transgenic and Gene Targeting Core at the University of California at San Diego.

REFERENCES

1. Kawai, T., and Akira, S. (2010) The role of pattern-recognition receptors in innate immunity: update on Toll-like receptors. *Nat. Immunol.* **11,** 373–384
2. Beutler, B. (2009) Microbe sensing, positive feedback loops, and the pathogenesis of inflammatory diseases. *Immunol. Rev.* **227,** 248–263
3. Schenten, D., and Medzhitov, R. (2011) The control of adaptive immune responses by the innate immune system. *Adv. Immunol.* **109,** 87–124
4. Sadler, A. J., and Williams, B. R. (2008) Interferon-inducible antiviral effectors. *Nat. Rev. Immunol.* **8,** 559–568

5. Lund, E. G., Kerr, T. A., Sakai, J., Li, W. P., and Russell, D. W. (1998) cDNA cloning of mouse and human cholesterol 25-hydroxylases, polytopic membrane proteins that synthesize a potent oxysterol regulator of lipid metabolism. *J. Biol. Chem.* **273,** 34316–34327
6. Bauman, D. R., Bitmansour, A. D., McDonald, J. G., Thompson, B. M., Liang, G., and Russell, D. W. (2009) 25-Hydroxycholesterol secreted by macrophages in response to Toll-like receptor activation suppresses immunoglobulin A production. *Proc. Natl. Acad. Sci. U.S.A.* **106,** 16764–16769
7. Dennis, E. A., Deems, R. A., Harkewicz, R., Quehenberger, O., Brown, H. A., Milne, S. B., Myers, D. S., Glass, C. K., Hardiman, G., Reichart, D., Merrill, A. H., Jr., Sullards, M. C., Wang, E., Murphy, R. C., Raetz, C. R., Garrett, T. A., Guan, Z., Ryan, A. C., Russell, D. W., McDonald, J. G., Thompson, B. M., Shaw, W. A., Sud, M., Zhao, Y., Gupta, S., Maurya, M. R., Fahy, E., and Subramaniam, S. (2010) A mouse macrophage lipidome. *J. Biol. Chem.* **285,** 39976–39985
8. Radhakrishnan, A., Ikeda, Y., Kwon, H. J., Brown, M. S., and Goldstein, J. L. (2007) Sterol-regulated transport of SREBPs from endoplasmic reticulum to Golgi: oxysterols block transport by binding to Insig. *Proc. Natl. Acad. Sci. U.S.A.* **104,** 6511–6518
9. Venkateswaran, A., Repa, J. J., Lobaccaro, J. M., Bronson, A., Mangelsdorf, D. J., and Edwards, P. A. (2000) Human white/murine ABC8 mRNA levels are highly induced in lipid-loaded macrophages. A transcriptional role for specific oxysterols. *J. Biol. Chem.* **275,** 14700–14707
10. Yi, T., Wang, X., Kelly, L. M., An, J., Xu, Y., Sailer, A. W., Gustafsson, J. A., Russell, D. W., and Cyster, J. G. (2012) Oxysterol gradient generation by lymphoid stromal cells guides activated B cell movement during humoral responses. *Immunity* **37,** 535–548
11. Blanc, M., Hsieh, W. Y., Robertson, K. A., Kropp, K. A., Forster, T., Shui, G., Lacaze, P., Watterson, S., Griffiths, S. J., Spann, N. J., Meljon, A., Talbot, S., Krishnan, K., Covey, D. F., Wenk, M. R., Craigon, M., Ruzsics, Z., Haas, J., Angulo, A., Griffiths, W. J., Glass, C. K., Wang, Y., and Ghazal, P. (2013) The transcription factor STAT-1 couples macrophage synthesis of 25-hydroxycholesterol to the interferon antiviral response. *Immunity* **38,** 106–118
12. Liu, S. Y., Aliyari, R., Chikere, K., Li, G., Marsden, M. D., Smith, J. K., Pernet, O., Guo, H., Nusbaum, R., Zack, J. A., Freiberg, A. N., Su, L., Lee, B., and Cheng, G. (2013) Interferon-inducible cholesterol-25-hydroxylase broadly inhibits viral entry by production of 25-hydroxycholesterol. *Immunity* **38,** 92–105
13. Wek, R. C., Jiang, H. Y., and Anthony, T. G. (2006) Coping with stress: eIF2 kinases and translational control. *Biochem. Soc. Trans.* **34,** 7–11
14. Donnelly, N., Gorman, A. M., Gupta, S., and Samali, A. (2013) The eIF2α kinases: their structures and functions. *Cell. Mol. Life Sci.* **70,** 3493–3511
15. Harding, H. P., Novoa, I., Zhang, Y., Zeng, H., Wek, R., Schapira, M., and Ron, D. (2000) Regulated translation initiation controls stress-induced gene expression in mammalian cells. *Mol. Cell* **6,** 1099–1108
16. Dey, S., Baird, T. D., Zhou, D., Palam, L. R., Spandau, D. F., and Wek, R. C. (2010) Both transcriptional regulation and translational control of ATF4 are central to the integrated stress response. *J. Biol. Chem.* **285,** 33165–33174
17. Zhang, K., and Kaufman, R. J. (2008) From endoplasmic-reticulum stress to the inflammatory response. *Nature* **454,** 455–462
18. Zinszner, H., Kuroda, M., Wang, X., Batchvarova, N., Lightfoot, R. T., Remotti, H., Stevens, J. L., and Ron, D. (1998) CHOP is implicated in programmed cell death in response to impaired function of the endoplasmic reticulum. *Genes Dev.* **12,** 982–995
19. Dabo, S., and Meurs, E. F. (2012) dsRNA-dependent protein kinase PKR and its role in stress, signaling and HCV infection. *Viruses* **4,** 2598–2635
20. García, M. A., Gil, J., Ventoso, I., Guerra, S., Domingo, E., Rivas, C., and Esteban, M. (2006) Impact of protein kinase PKR in cell biology: from antiviral to antiproliferative action. *Microbiol. Mol. Biol. Rev.* **70,** 1032–1060
21. Iwasaki, A. (2012) A virological view of innate immune recognition. *Annu. Rev. Microbiol.* **66,** 177–196
22. Repa, J. J., Liang, G., Ou, J., Bashmakov, Y., Lobaccaro, J. M., Shimomura, I., Shan, B., Brown, M. S., Goldstein, J. L., and Mangelsdorf, D. J. (2000) Regulation of mouse sterol regulatory element-binding protein-1c gene (SREBP-1c) by oxysterol receptors, LXRα and LXRβ. *Genes Dev.* **14,** 2819–2830
23. Valledor, A. F., Hsu, L. C., Ogawa, S., Sawka-Verhelle, D., Karin, M., and Glass, C. K. (2004) Activation of liver X receptors and retinoid X receptors prevents bacterial-induced macrophage apoptosis. *Proc. Natl. Acad. Sci. U.S.A.* **101,** 17813–17818
24. Engelking, L. J., Liang, G., Hammer, R. E., Takaishi, K., Kuriyama, H., Evers, B. M., Li, W. P., Horton, J. D., Goldstein, J. L., and Brown, M. S. (2005) Schoenheimer effect explained–Feedback regulation of cholesterol synthesis in mice mediated by Insig proteins. *J. Clin. Invest.* **115,** 2489–2498
25. Zhang, P., McGrath, B. C., Reinert, J., Olsen, D. S., Lei, L., Gill, S., Wek, S. A., Vattem, K. M., Wek, R. C., Kimball, S. R., Jefferson, L. S., and Cavener, D. R. (2002) The GCN2 eIF2α kinase is required for adaptation to amino acid deprivation in mice. *Mol. Cell. Biol.* **22,** 6681–6688
26. Heinz, S., Benner, C., Spann, N., Bertolino, E., Lin, Y. C., Laslo, P., Cheng, J. X., Murre, C., Singh, H., and Glass, C. K. (2010) Simple combinations of lineage-determining transcription factors prime cis-regulatory elements required for macrophage and B cell identities. *Mol. Cell* **38,** 576–589
27. Ghisletti, S., Huang, W., Ogawa, S., Pascual, G., Lin, M. E., Willson, T. M., Rosenfeld, M. G., and Glass, C. K. (2007) Parallel SUMOylation-dependent pathways mediate gene- and signal-specific transrepression by LXRs and PPARγ. *Mol. Cell* **25,** 57–70
28. Heiman, M., Schaefer, A., Gong, S., Peterson, J. D., Day, M., Ramsey, K. E., Suárez-Fariñas, M., Schwarz, C., Stephan, D. A., Surmeier, D. J., Greengard, P., and Heintz, N. (2008) A translational profiling approach for the molecular characterization of CNS cell types. *Cell* **135,** 738–748
29. Lam, M. T., Cho, H., Lesch, H. P., Gosselin, D., Heinz, S., Tanaka-Oishi, Y., Benner, C., Kaikkonen, M. U., Kim, A. S., Kosaka, M., Lee, C. Y., Watt, A., Grossman, T. R., Rosenfeld, M. G., Evans, R. M., and Glass, C. K. (2013) Rev-Erbs repress macrophage gene expression by inhibiting enhancer-directed transcription. *Nature* **498,** 511–515
30. Huang da, W., Sherman, B. T., and Lempicki, R. A. (2009) Systematic and integrative analysis of large gene lists using DAVID bioinformatics resources. *Nat. Protoc.* **4,** 44–57
31. Dennis, G., Jr., Sherman, B. T., Hosack, D. A., Yang, J., Gao, W., Lane, H. C., and Lempicki, R. A. (2003) DAVID: Database for annotation, visualization, and integrated discovery. *Genome Biol.* **4,** P3
32. Morello, C. S., Kelley, L. A., Munks, M. W., Hill, A. B., and Spector, D. H. (2007) DNA immunization using highly conserved murine cytomegalovirus genes encoding homologs of human cytomegalovirus UL54 (DNA polymerase) and UL105 (helicase) elicits strong CD8 T-cell responses and is protective against systemic challenge. *J. Virol.* **81,** 7766–7775
33. González Armas, J. C., Morello, C. S., Cranmer, L. D., and Spector, D. H. (1996) DNA immunization confers protection against murine cytomegalovirus infection. *J. Virol.* **70,** 7921–7928
34. Mungrue, I. N., Pagnon, J., Kohannim, O., Gargalovic, P. S., and Lusis, A. J. (2009) CHAC1/MGC4504 is a novel proapoptotic component of the unfolded protein response, downstream of the ATF4-ATF3-CHOP cascade. *J. Immunol.* **182,** 466–476
35. Budt, M., Niederstadt, L., Valchanova, R. S., Jonjić, S., and Brune, W. (2009) Specific inhibition of the PKR-mediated antiviral response by the murine cytomegalovirus proteins m142 and m143. *J. Virol.* **83,** 1260–1270
36. Marcinowski, L., Lidschreiber, M., Windhager, L., Rieder, M., Bosse, J. B., Rädle, B., Bonfert, T., Györy, I., de Graaf, M., Prazeres da Costa, O., Rosenstiel, P., Friedel, C. C., Zimmer, R., Ruzsics, Z., and Dölken, L. (2012) Real-time transcriptional profiling of cellular and viral gene expression during lytic cytomegalovirus infection. *PLoS Pathog.* **8,** e1002908
37. Brown, M. S., and Goldstein, J. L. (2009) Cholesterol feedback: from Schoenheimer's bottle to Scap's MELADL. *J. Lipid Res.* **50,** S15–S27
38. Hershey, J. W. (1989) Protein phosphorylation controls translation rates. *J. Biol. Chem.* **264,** 20823–20826
39. Wek, R. C., and Cavener, D. R. (2007) Translational control and the unfolded protein response. *Antioxid. Redox Signal.* **9,** 2357–2371
40. Sasmono, R. T., Oceandy, D., Pollard, J. W., Tong, W., Pavli, P., Wainwright, B. J., Ostrowski, M. C., Himes, S. R., and Hume, D. A. (2003) A macrophage colony-stimulating factor receptor-green fluorescent protein transgene is expressed throughout the mononuclear phagocyte system of

the mouse. *Blood* **101,** 1155–1163
41. Han, J., Back, S. H., Hur, J., Lin, Y. H., Gildersleeve, R., Shan, J., Yuan, C. L., Krokowski, D., Wang, S., Hatzoglou, M., Kilberg, M. S., Sartor, M. A., and Kaufman, R. J. (2013) ER-stress-induced transcriptional regulation increases protein synthesis leading to cell death. *Nat. Cell Biol.* **15,** 481–490
42. Horton, J. D., Shah, N. A., Warrington, J. A., Anderson, N. N., Park, S. W., Brown, M. S., and Goldstein, J. L. (2003) Combined analysis of oligonucleotide microarray data from transgenic and knockout mice identifies direct SREBP target genes. *Proc. Natl. Acad. Sci. U.S.A.* **100,** 12027–12032
43. Berlanga, J. J., Ventoso, I., Harding, H. P., Deng, J., Ron, D., Sonenberg, N., Carrasco, L., and de Haro, C. (2006) Antiviral effect of the mammalian translation initiation factor 2α kinase GCN2 against RNA viruses. *EMBO J.* **25,** 1730–1740
44. Harding, H. P., Zhang, Y., Zeng, H., Novoa, I., Lu, P. D., Calfon, M., Sadri, N., Yun, C., Popko, B., Paules, R., Stojdl, D. F., Bell, J. C., Hettmann, T., Leiden, J. M., and Ron, D. (2003) An integrated stress response regulates amino acid metabolism and resistance to oxidative stress. *Mol. Cell* **11,** 619–633
45. Ye, J., Kumanova, M., Hart, L. S., Sloane, K., Zhang, H., De Panis, D. N., Bobrovnikova-Marjon, E., Diehl, J. A., Ron, D., and Koumenis, C. (2010) The GCN2-ATF4 pathway is critical for tumour cell survival and proliferation in response to nutrient deprivation. *EMBO J.* **29,** 2082–2096
46. Lee, J. I., Dominy, J. E., Jr., Sikalidis, A. K., Hirschberger, L. L., Wang, W., and Stipanuk, M. H. (2008) HepG2/C3A cells respond to cysteine deprivation by induction of the amino acid deprivation/integrated stress response pathway. *Physiol. Genomics* **33,** 218–229
47. Suraweera, A., Münch, C., Hanssum, A., and Bertolotti, A. (2012) Failure of amino acid homeostasis causes cell death following proteasome inhibition. *Mol. Cell* **48,** 242–253
48. Brüne, B., Dehne, N., Grossmann, N., Jung, M., Namgaladze, D., Schmid, T., von Knethen, A., and Weigert, A. (2013) Redox control of inflammation in macrophages. *Antioxid. Redox Signal.* **19,** 595–637
49. Gupte, A. A., Lyon, C. J., and Hsueh, W. A. (2013) Nuclear factor (Erythroid-derived 2)-like-2 factor (Nrf2), a key regulator of the antioxidant response to protect against atherosclerosis and nonalcoholic steatohepatitis. *Curr. Diabetes Rep.* **13,** 362–371
50. Lange, Y., and Steck, T. L. (1994) Cholesterol homeostasis. Modulation by amphiphiles. *J. Biol. Chem.* **269,** 29371–29374
51. Tabas, I., Rosoff, W. J., and Boykow, G. C. (1988) Acyl coenzyme A:cholesterol acyl transferase in macrophages utilizes a cellular pool of cholesterol oxidase-accessible cholesterol as substrate. *J. Biol. Chem.* **263,** 1266–1272
52. Hullin-Matsuda, F., Tomishige, N., Sakai, S., Ishitsuka, R., Ishii, K., Makino, A., Greimel, P., Abe, M., Laviad, E. L., Lagarde, M., Vidal, H., Saito, T., Osada, H., Hanada, K., Futerman, A. H., and Kobayashi, T. (2012) Limonoid compounds inhibit sphingomyelin biosynthesis by preventing CERT protein-dependent extraction of ceramides from the endoplasmic reticulum. *J. Biol. Chem.* **287,** 24397–24411
53. Ridgway, N. D. (2000) Interactions between metabolism and intracellular distribution of cholesterol and sphingomyelin. *Biochim. Biophys. Acta* **1484,** 129–141
54. Li, X., Gulbins, E., and Zhang, Y. (2012) Oxidative stress triggers CA-dependent lysosome trafficking and activation of acid sphingomyelinase. *Cell. Physiol. Biochem.* **30,** 815–826
55. Ridgway, N. D. (1995) 25-Hydroxycholesterol stimulates sphingomyelin synthesis in Chinese hamster ovary cells. *J. Lipid Res.* **36,** 1345–1358
56. Guo, F., and Cavener, D. R. (2007) The GCN2 eIF2α kinase regulates fatty-acid homeostasis in the liver during deprivation of an essential amino acid. *Cell Metab.* **5,** 103–114
57. Lu, S. C. (2013) Glutathione synthesis. *Biochim. Biophys. Acta* **1830,** 3143–3153
58. Meister, A. (1988) Glutathione metabolism and its selective modification. *J. Biol. Chem.* **263,** 17205–17208
59. Wilkins, C., and Gale, M., Jr. (2013) Sterolizing innate immunity. *Immunity* **38,** 3–5
60. Lorizate, M., and Kräusslich, H. G. (2011) Role of lipids in virus replication. *Cold Spring Harbor Perspect. Biol.* **3,** a004820
61. Waheed, A. A., and Freed, E. O. (2009) Lipids and membrane microdomains in HIV-1 replication. *Virus Res.* **143,** 162–176
62. Chan, R. B., Tanner, L., and Wenk, M. R. (2010) Implications for lipids during replication of enveloped viruses. *Chem. Phys. Lipids* **163,** 449–459
63. Cláudio, N., Dalet, A., Gatti, E., and Pierre, P. (2013) Mapping the crossroads of immune activation and cellular stress response pathways. *EMBO J.* **32,** 1214–1224
64. Walsh, D., and Mohr, I. (2011) Viral subversion of the host protein synthesis machinery. *Nat. Rev. Microbiol.* **9,** 860–875
65. del Pino, J., Jiménez, J. L., Ventoso, I., Castelló, A., Muñoz-Fernández, M. Á., de Haro, C., and Berlanga, J. J. (2012) GCN2 has inhibitory effect on human immunodeficiency virus-1 protein synthesis and is cleaved upon viral infection. *PLoS One* **7,** e47272
66. Tattoli, I., Sorbara, M. T., Vuckovic, D., Ling, A., Soares, F., Carneiro, L. A., Yang, C., Emili, A., Philpott, D. J., and Girardin, S. E. (2012) Amino acid starvation induced by invasive bacterial pathogens triggers an innate host defense program. *Cell Host Microbe* **11,** 563–575
67. Won, S., Eidenschenk, C., Arnold, C. N., Siggs, O. M., Sun, L., Brandl, K., Mullen, T. M., Nemerow, G. R., Moresco, E. M., and Beutler, B. (2012) Increased susceptibility to DNA virus infection in mice with a GCN2 mutation. *J. Virol.* **86,** 1802–1808